Low dimensional magnetism in the trirutile tantalates Co $_{1-x}$ Mg $_x$ Ta $_2$ O $_6$ with weak-ferromagnetic features

Cite as: J. Appl. Phys. **125**, 033904 (2019); https://doi.org/10.1063/1.5063338 Submitted: 26 September 2018 . Accepted: 02 January 2019 . Published Online: 18 January 2019

R. Baral 📵, H. S. Fierro, L. M. Martinez, S. R. Singamaneni 📵, and H. S. Nair 📵







ARTICLES YOU MAY BE INTERESTED IN

Ti-doped YMnO₃: Magnetic and thermal studies at low temperature and dielectric properties at high temperature

Journal of Applied Physics 125, 034102 (2019); https://doi.org/10.1063/1.5055228

Magnetization behavior of electrochemically synthesized Co₂MnSn full Heusler alloy nanowire arrays

Journal of Applied Physics 125, 034302 (2019); https://doi.org/10.1063/1.5058066

Magnetostriction induced by crystallographic orientation and morphological alignment in a TbFe₂-based alloy

Journal of Applied Physics 125, 033901 (2019); https://doi.org/10.1063/1.5080799

Lock-in Amplifiers up to 600 MHz







Low dimensional magnetism in the trirutile tantalates Co_{1-x}Mg_xTa₂O₆ with weak-ferromagnetic features

Cite as: J. Appl. Phys. 125, 033904 (2019); doi: 10.1063/1.5063338 Submitted: 26 September 2018 · Accepted: 2 January 2019 · Published Online: 18 January 2019







R. Baral, DH. S. Fierro, L. M. Martinez, S. R. Singamaneni, Dand H. S. Nair



AFFILIATIONS

Department of Physics, University of Texas at El Paso, 500 West University Avenue, El Paso, Texas 79968, USA

ABSTRACT

The magnetic properties of the low-dimensional trirutile tantalates $Co_{1-x}Mg_xTa_2O_6$ [x = 0.0, 0.1, 0.3, 0.5, 0.7, 1.0] are reported in this paper. $CoTa_2O_6$ is an antiferromagnet with a transition temperature at $T_N = 6.6$ K, while showing a very broad peak in the magnetic susceptibility at \approx 12 K owing to the low dimensionality of the magnetic interactions. In our study, where Mg is introduced at the Co position, we see the disappearance of the broad transition for high values of x. For the x = 0.1 composition, three transitions are observed in the magnetization at 28 K, 6 K, and 3.3 K. Our analysis of magnetization data using the anisotropic Heisenberg and the Ising models for spin chains points out that the magnetic interactions in Co_{1-x}Mg_xTa₂O₆ are indeed low dimensional. Field-induced metamagnetic transitions are observed in the case of x = 0 and x = 0.1 compositions of $Co_{1-x}Mg_xTa_2O_6$, which are evident in the magnetization isotherms at T=2 K. Interestingly, we find that with progressive doping up to x = 0.5 and 0.7, we obtain higher magnetization pointing to the possibility of weak-ferromagnetism. This might point toward the formation of single-chain magnets, which opens up a new possibility in low dimensional oxides for spintronics applications.

Published under license by AIP Publishing, https://doi.org/10.1063/1.5063338

I. INTRODUCTION

Low dimensional magnetic materials that have Ising or Heisenberg interactions along chains of magnetic moments are exotic systems to study the possibility of spin-based topological current transport. Low dimensional magnets can form the building blocks of magnetic textures formed by systematically stacking Ising and Heisenberg ferromagnets, or they could be attached to nano-substrates to create spins that have exotic quantum-mechanical phases. One class of low dimensional magnets that have received less attention is the trirutiles of the general formula MTa_2O_6 , where M = transition metal (Cu, Ni, Co, Mn, Fe).²⁻¹² The trirutile structure of these compounds is derived from the rutile structure. In the former, chemical ordering of the divalent and the pentavalent cations leads to a tetragonal structure with the c axis length being tripled. An interesting member in this family of low dimensional magnets is $\overline{\text{CoTa}_2}\text{O}_6$. 4,10,11,13,14 The presence of $\overline{\text{Co}^{2+}}$ in the octahedral environment forming chains along the c axis makes it an interesting candidate to test the physics of low dimensionality. An antiferromagnetic transition is detected below 6.6 K in CoTa₂O₆, which displays a broad feature in the

magnetization centered at around 12 K which arises from the low dimensionality of magnetic interactions.^{4,10} The specific heat of CoTa₂O₆ had been studied in the past and was analyzed using the assumption of an Ising net of magnetic moments.^{4,11} One of the earliest experimental studies of the macroscopic magnetic properties of MTa₂O₆ (M = Co, Ni, Fe) identified these compounds as antiferromagnets, where CoTa2O6 was found to have an effective moment of $5.31\mu_B$ and a Curie-Weiss temperature of -35 K.¹³ Recent studies on the single crystals of CoTa₂O₆ have shown significant anisotropy effects on magnetic susceptibility and thermal expansion.4 According to some reports, the magnetic lattice of MTa₂O₆ consists of the M²⁺ ions forming square-planar layers stacked along the c axis. ^{11,16} A neutron diffraction study observed an antiferromagnetic structure with the propagation vector $(\pm \frac{1}{4}, \pm \frac{1}{4})$, where the magnetic moments lie entirely on the Co-O planes. An earlier neutron diffraction study of CoTa₂O₆ ascribed the observed magnetic reflections to a propagation vector $(\frac{1}{4}, \frac{1}{4}, \frac{1}{4})$ and used a two-cone axis helical spin structure to explain the magnetic structure.¹⁴ So, essentially, a two dimensional magnetic structure was ascribed to these compounds by several studies and the

magnetic exchange paths have been identified as the M-O-O-M chains along the (110) crystallographic direction. Alternatively, one could look at the magnetic structure consisting of chains of M^{2+} along the c axis where the chains are separated by the non-magnetic Ta atoms. This quasi onedimensional nature of the magnetic chains was recently provided with a stronger footing through careful specific heat measurements on single crystals of CoTa₂O₆ along different crystallographic axes.⁴ The fact that the peak in specific heat at the transition temperature was seen to split into two, when the external magnetic field was applied along [110] or [1 $\bar{1}$ 0], could be understood only by assuming a chain-like structure. The crystal structure of trirutile CoTa₂O₆ is given in Fig. 1, along with the planar network of Co atoms that forms the magnetic lattice. It is these structural features that lead to the magnetic anisotropies and low-dimensional magnetism. The presence of a shortrange magnetic order well above T_N (the antiferromagnetic transition) has been documented for many of the trirutiles, which have a one-dimensional magnetic arrangement of spins with weak interaction. 12,17 In this context of low-dimensional chain-like structures that the trirutiles form, exotic phases of magnets like the Luttinger liquids, dimerization, spin-Peierls transitions, and spin liquid states can arise depending on the values of the nearest-neighbour (J₁), the next-nearest-neighbour (J_2) , and the anisotropy parameter (Δ) .¹⁸

In the present paper, we investigate the low-dimensional magnetism in a series of compounds Co_{1-x}Mg_xTa₂O₆ derived from the trirutile compound CoTa₂O₆ through progressive dilution of the Co lattice with Mg. It is clear that the early studies on CoTa₂O₆ approached the magnetic structure of this compound as a Ising net with a two dimensional structure, 11 which is supported by recent neutron diffraction experiments. 16 The magnetic interactions in CoTa_2O_6 have

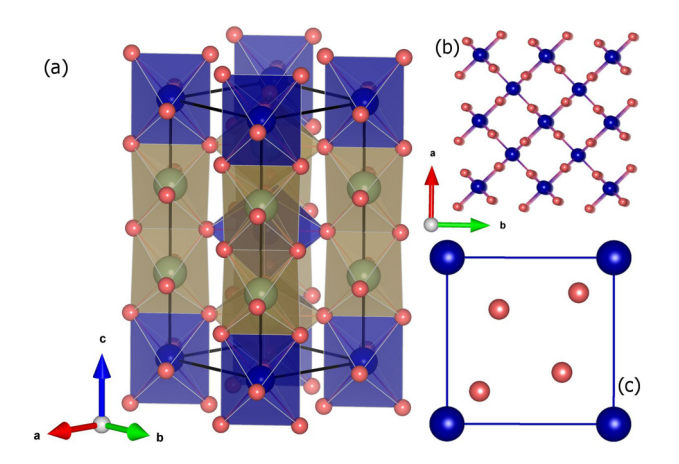


FIG. 1. A schematic diagram of the crystal structure of CoTa₂O₆ in P4₂/mnm space group. (a) A polyhedral network where the blue octahedra are the CoO6 units. The Co-chains along the c axis can be seen. (b) and (c) The square planar structure of the Co magnetic lattice. The structure diagrams were prepared using VESTA.

been ascribed to a two dimensional square planar network of Co moments or to the one dimensional Ising or anisotropic Heisenberg-like chains which form in the [110] direction of the tetragonal cell. Through Mg dilution at the Co lattice, we attempt to probe the possibility of diluting the chains with the idea of forming single chain magnets which can be potential candidates for spintronics. Sr_{4-x}Ca_xMn₂CoO₉ is one such oxide which has recently been experimentally shown to possess the features of single-chain magnetism in triangular spin chains.²

II. EXPERIMENTAL METHODS

The polycrystalline samples used in the present study were prepared following a standard solid state reaction method as described in a previous report on CoTa₂O₆.² The precursors Co₂O₃, MgO, and Ta₂O₅ (≥4N purity) were used as purchased from Fisher Scientific. After mixing the stoichiometric amount of precursors in a mortar and pestle, the mixed and ground powders were heated at 1350 °C for 12 h. The process of heating was repeated four times with intermediate grinding to make sure phase-pure samples of $Co_{1-x}Mg_xTa_2O_6$ for x = 0.0, 0.1, 0.3, 0.5, 0.7, and 1.0. Powder x ray diffraction (PXRD) patterns of the Co_{1-x}Mg_xTa₂O₆ compositions were recorded in a Rigaku MiniFlex diffractometer with a Cu target employing the wavelength 1.548 Å. The PXRD patterns were analyzed using the Rietveld method²⁵ coded in Fullprof Suite.²⁶ Magnetic measurements were collected using the ACMS option of a Physical Property Measurement System (PPMS) from Quantum Design. The dc extraction method was used to measure the dc magnetic susceptibility in zero field cooled (ZFC) and field cooled (FC) protocols. Magnetization isotherms were recorded in the field range of $\pm 7\,\mathrm{T}$. Magnetization as a function of temperature was recorded in the temperature range 2 K-300 K.

III. RESULTS AND DISCUSSION

The crystal structure of CoTa₂O₆ in the trirutile phase is attributed to the $P4_2/mnm$ space group similar to the tapiolite compound FeTa₂O₆. 14,24,27 This class of compounds are known for antiferromagnetism arising from low-dimensional chainlike structures that the transition metal forms. $^{5,6,10,11,28-30}$ The compositions of Co_{1-x}Mg_xTa₂O₆ also belong to the trirutile P42/mnm space group similar to the end-member compounds CoTa₂O₆ and MgTa₂O₆. Figures 2(a)-2(d) show the PXRD patterns collected at T = 300 K for $Co_{1-x}Mg_xTa_2O_6$ for x = 0, 0.1, 0.5, and 1. The PXRD patterns of the other compositions are similar and hence not presented. The black solid lines in the figures are the Rietveld fits using the space group P42/mnm, which provided satisfactory fits. The refined lattice parameters for all the compositions of Co_{1-x}Mg_xTa₂O₆ are presented in Table I, which also include the refined atomic coordinates for CoTa₂O₆. In the inset of Fig. 2(d), the evolution of the lattice parameters, a and c, as a function of the Mg-content, x is shown. In the case of a, a nearly linear relationship is found where the lattice constant decreases with

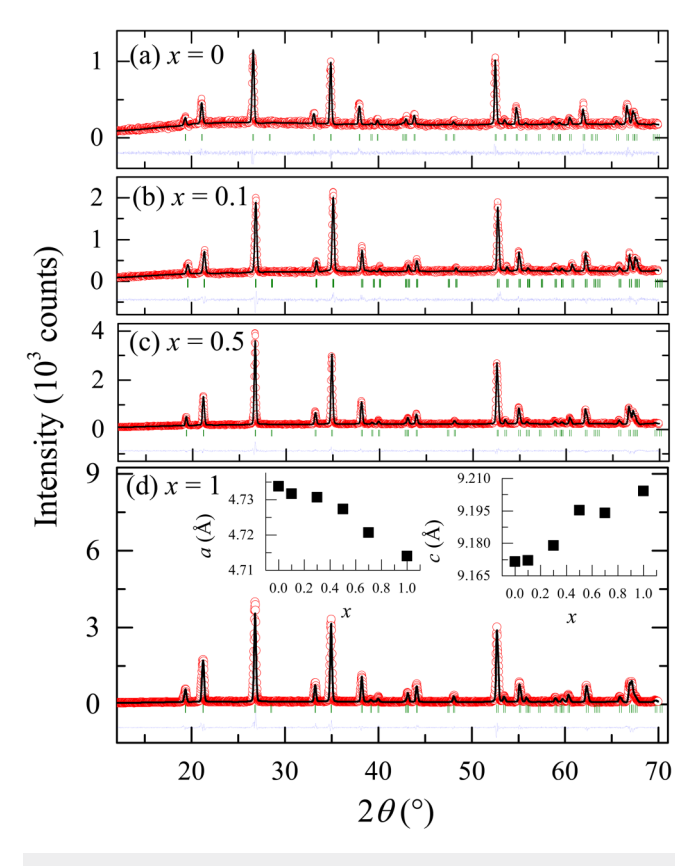


FIG. 2. (a)–(d) The Rietveld refinement patterns (black solid line) plotted on the top of the experimental PXRD (red circles) of $Co_{1-x}Mg_xTa_2O_6$ compounds shown for $x=0,\,0.1,\,0.5$, and 1.0. The difference patterns are shown in blue and the Bragg peaks as vertical tick marks. The variation of lattice parameters as a function of Mg content, x, are shown in the inset of (d) for a (left inset) and c (right inset). The error bars were comparable to the size of the data markers.

TABLE I. The refined lattice parameters of the different compositions of the $Co_{1-x}Mg_xTa_2O_6$ series studied in the present paper. The goodness-of-fit parameter is indicated for each composition. The atomic parameters for $CoTa_2O_6$ which were used for the refinement are shown.

	a (Å)		c (Å)	χ^2
CoTa ₂ O ₆	4.7337(2)		9.1715(6)	1.18
x = 0.1	4.7316(2)		9.1721(4)	1.79
x = 0.3	4.7306(2)		9.1790(4)	1.49
x = 0.5	4.7273(1)		9.1953(3)	1.43
x = 0.7	4.7206(1)		9.1941(3)	1.40
MgTa ₂ O ₆	4.7139(2)		9.2042(3)	2.33
Atom	Wyckoff pos.	х	у	Z

Atom	Wyckoff pos.	X	У	Z
Со	2a	0.0	0.0	0.0
Ta	4e	0.0	0.0	0.33090
0	4 <i>f</i>	0.31095	0.31095	0.0
0	8 <i>j</i>	0.29810	0.29810	0.33472

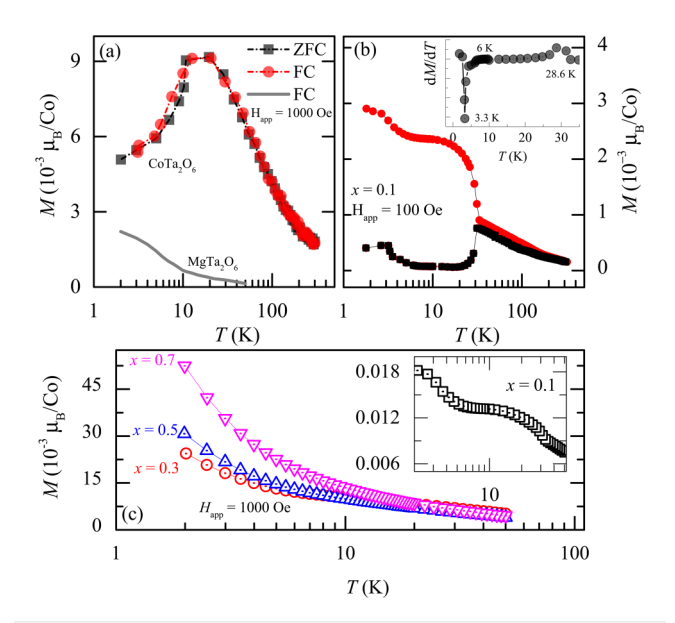


FIG. 3. (a) The magnetization M(T) of $\mathrm{Co_{1-x}Mg_xTa_2O_6}$ in ZFC and FC protocols measured at $H_{\mathrm{app}}=1000$ Oe, plotted as a function of temperature. The paramagnetic response of $\mathrm{MgTa_2O_6}$ is also presented in the same graph. (b) The ZFC and FC plots of M(T) (at $H_{\mathrm{app}}=100$ Oe) of $\mathrm{Co_{0.9}Mg_{0.1}Ta_2O_6}$ which shows a significant irreversibility at 30 K. Further anomalies are present at low temperatures. The inset shows the derivative dM/dT showing the three anomalies present in the case of x=0.1. (c) An enhancement in magnetism at low temperature is seen for x=0.5 and 0.7. The inset shows the FC curve of x=0.1 at $H_{\mathrm{app}}=1000$ Oe. Note that all curves are plotted in the semi-log axis.

increasing x. An opposite trend is observed for c; however, a weak anomaly is seen at x = 0.5.

The ZFC and FC arms of the M(T) curve of CoTa₂O₆ are shown in Fig. 3(a). The magnetization curves were recorded at an applied field, $H_{app} = 1000$ Oe. A broad feature is present in the magnetization response at \approx 12 K which shows no bifurcation between the ZFC and FC curves. As a comparison, the FC M(T) response of the non-magnetic analogue MgTa₂O₆ (in the temperature range 2 K-50 K), which presents a purely paramagnetic response, is also presented in the same graph. The enhancement of paramagnetic susceptibility seen at low temperatures could be attributed to the presence of minute defects or impurities that are polarized in the process of field-cooling. The broad magnetic anomaly that we have observed is reported in the previous works on polycrystalline CoTa₂O₆¹⁶ and in oriented single crystals. It is an unmistakable sign of the low dimensionality of the magnetic interactions in the Co lattice. The change in slope that occurs at $T_{N} \approx 6\,\text{K}$ is adjudged by the antiferromagnetic transition in the Co lattice.

The Curie-Weiss fit was administered to the high temperature region of M(T) of all the compositions. The temperature range $150\,\mathrm{K}{-}320\,\mathrm{K}$ was selected for the fits. The Curie-Weiss fit in the case of transition metal atoms is prone to give misleading values if the crystal field terms are not

properly taken into account and hence a "range-of-fit" analysis is recommended, especially in cases of complex magnetic systems.³¹ Since in the present case we have Co in an octahedral environment, which is prone to have high temperature crystal field effects, we have performed the Curie-Weiss fit in different temperature ranges above 150 K and obtained an average value of the effective moment as $4.9(2) \mu_B$ and $\theta_p = -50$ K. This value indicates Co^{2+} in the S = 3/2 state. A significantly lower value in the range of 2–2.7 μ_B is observed in the case of Co²⁺ if it is in a low-spin state⁴ The effective moment values of all the compositions of Co_{1-x}Mg_xTa₂O₆ are presented in Table II. A nonlinear trend in the values of $\mu_{\rm eff}$ is seen where a minimum is observed for Co_{0.5}Mg_{0.5}Ta₂O₆, and further a slight increase for Co_{0.3}Mg_{0.7}Ta₂O₆. We do not have any convincing experimental proof to support this observation. However, the anomalies seen in the lattice parameters around Co_{0.5}Mg_{0.5}Ta₂O₆ and Co_{0.3}Mg_{0.7}Ta₂O₆ might be related to this. Another possibility is a transformation of part of the cobalt ions into a low-spin state. The ZFC and FC curves of M(T) of $Co_{0.9}Mg_{0.1}Ta_2O_6$ recorded at $H_{app} = 100 Oe$ is presented in panel (b) of Fig. 3. Remarkable irreversibility is seen in the ZFC and FC arms of the magnetization, where a bifurcation happens at $T_{N1} = 28.6 \, \text{K}$. Further, additional anomalies are present in the low temperature at $T_{N2}=6\,\mathrm{K}$ and at $T_{\rm N3} = 3.3$ K. The exact temperature values of the anomalies were determined from the derivative of magnetization with respect to temperature, dM/dT, as shown in the inset of Fig. 3(b). To the best of our knowledge, these anomalies in the x = 0.1 compound are reported for the first time. No thermal hysteresis between the FC-warming and FC-cooling curves (not presented) was observed, thereby ruling out any firstorder effects due to structural or magnetic disorder in the system. With the application of 1000 Oe, the anomalies are seen to smoothen out; however, broad features were seen to remain [inset of Fig. 3(c)]. It should be pointed out here that nano-sized impurities of Co₃O₄, if formed as a minority phase in the compound, can influence the magnetic properties.³

TABLE II. The effective paramagnetic moment $(\mu_{\rm eff})$, Curie-Weiss temperature (θ_p) , and the maximum magnetic moment $(M_{\rm max})$ estimated from the Curie-Weiss analysis of inverse magnetic susceptibility at high temperatures. The values of g and exchange parameter estimated using the Ising $(J_{nn}^{\rm I})$ and Bonner-Fisher $(J_{nn}^{\rm BF})$ fits are given in the lower section.

	μ_{eff} (μ_{B}/Co)	θ_p (K)	$M_{\rm max} \; (\mu_{\rm B}/{ m Co})$
x = 0.0	4.9(2)	-50(2)	0.45
x = 0.1	4.8(2)	-18(1)	0.54
x = 0.3	4.3(3)	-27(2)	0.52
x = 0.5	1.1(2)	-13(1)	0.53
x = 0.7	2.9(3)	-25(2)	0.75
	g	$J_{nn}^{l}(K)$	J_{nn}^{BF} (K)
x = 0.0	2.7(1)	-24	—15
x = 0.1	3.3(2)	-25	-18
x = 0.3	2.3(3)	-21	-16
x = 0.5	1.9(3)	-18	-13
x = 0.7	1.4(2)	-43	-10

From Table II, it can be seen that the $\mu_{\rm eff}$ and the θ_p are reduced compared to the x=0.0 compound. However, a predominant antiferromagnetic response is retained. As the Mg-content is further increased, the magnetic anomalies present in the x=0 and 0.1 compositions vanish for $x=0.3,\,0.5,\,$ and 0.7 which retain a paramagnetic-like response down to 2 K [see Fig. 3(c)]. There is a progressive enhancement of magnetization at low temperature with the increase in Mg-content. With progressive non-magnetic Mg in the Co lattice, the antiferromagnetism is destabilized along the chains giving way to ferromagnetic clusters.

The broad peak in the magnetization as seen in panel (a) of Fig. 3 is reminiscent of low dimensional (1 dimensional spin chains) spin compounds. In order to analyze the magnetization data, we have used two models in this paper: (i) Bonner-Fisher and (ii) Ising. As a first approach, the susceptibility is modeled after the Bonner Fisher model. 33,34 We have made use of the S = 1/2 infinite isotropic Heisenberg chain expression to model the magnetic susceptibility of the $\rm Co_{1-x}Mg_xTa_2O_6$ compounds. Consequently, the magnetic susceptibility was modeled as

$$\chi_{\rm BF} = \frac{Ng^2\mu_{\rm B}^2}{k_{\rm B}T} \left[\frac{0.25 + 0.14995x + 0.30094x^2}{1 + 1.9862x + 0.68854x^2 + 6.0626x^3} \right], \qquad \mbox{(1)}$$

with $x = |J|/k_BT$. The fits obtained using the Bonner-Fisher model is presented in Figs. 4(a)-4(c) in blue solid lines for

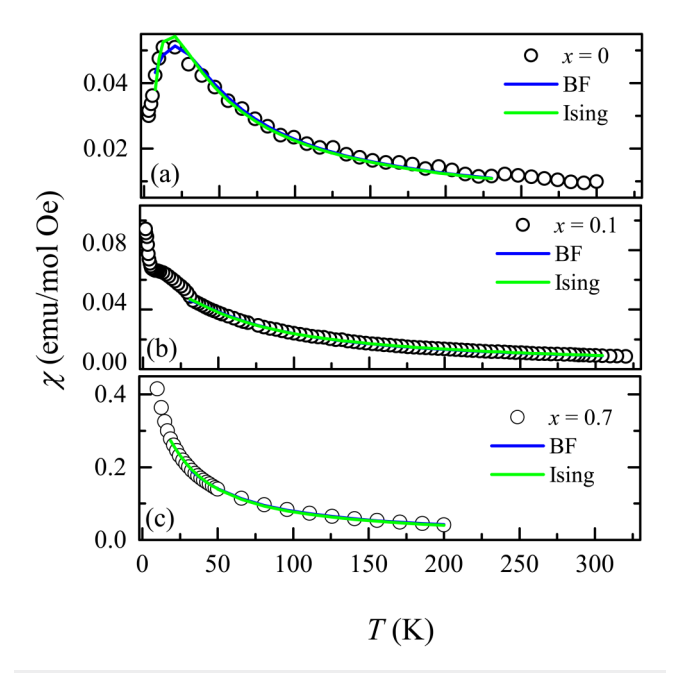


FIG. 4. The magnetic susceptibility, $\chi(T)$, of $Co_{1-x}Mg_xTa_2O_6$ compounds plotted in a semi-log axis along with the fits using the Ising model (green solid line) and Bonner-Fisher model (BF, blue solid line). The x=0, 0.1, and 0.7 cases are shown in (a), (b), and (c) respectively.

x=0, 0.1 and 0.7, respectively. Note that the broad peak in the case of x=0 is accounted for by the fit, although the model is most apt for a spin-half system. Another approach is to use a modified Ising model where the magnetic susceptibility of the single crystals of CoTa_2O_6 were well accounted for by using the susceptibility of S=1/2 dimers modeled by Carlin.^{2,34} The spin-half expression was adapted for the S=3/2 case of Co^{2+} as follows:

$$\chi_{\rm I} = \xi \left[\frac{e^{\frac{3J}{{\rm k_B} {\rm T}}} \left(2 + e^{\frac{2J}{{\rm k_B} {\rm T}}} + 8e^{\frac{3J}{{\rm k_B} {\rm T}}} + 9e^{\frac{6J}{{\rm k_B} {\rm T}}} \right)}{1 + 2e^{\frac{3J}{{\rm k_B} {\rm T}}} + e^{\frac{4J}{{\rm k_B} {\rm T}}} + e^{\frac{5J}{{\rm k_B} {\rm T}}} + 2e^{\frac{6J}{{\rm k_B} {\rm T}}} + e^{\frac{4J}{{\rm k_B} {\rm T}}}} \right], \tag{2}$$

where $\xi=\frac{Ng^2\mu_B^2}{2k_BT}$. The fit to the magnetic susceptibility of $Co_{1-x}Mg_xTa_2O_6$ using the Ising model is shown in Fig. 4 in the green solid line. Note that the quality of the fit is good and for x=0 compound, g=2.7(1) and $J/k_B=24\,\mathrm{K}$ are obtained which are comparable to the values obtained for g_\parallel , J_\parallel/k_B in the case of single crystals of $CoTa_2O_6$. In Fig. 4, the fits to other compositions x=0.1 and 0.7 are also shown. It should be noted here that the BF and Ising models for low dimensional systems are consistently described for spin-half systems and no extension of these models exist for high-S systems. We have hence used a similar approach as used by the authors in Ref. 2. A clear distinction between the goodness-of-fit for the two models could not be obtained using the present data on polycrystals. The fit parameters extracted from the analysis are shown in Table II.

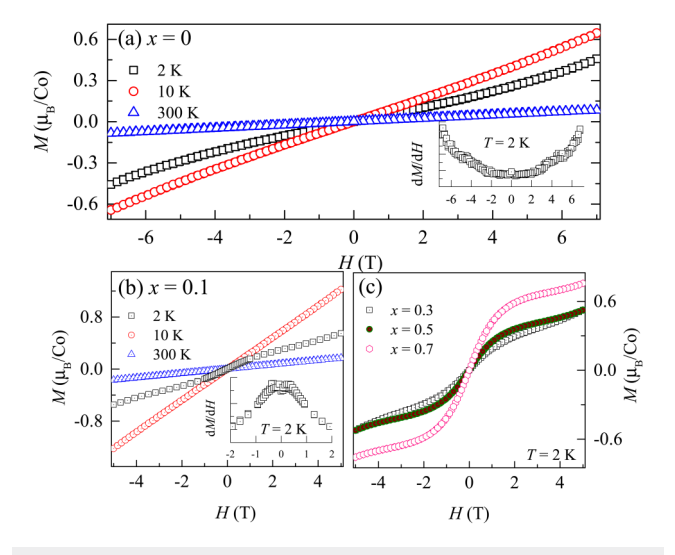


FIG. 5. (a) The magnetization isotherm, M(H), of $CoTa_2O_6$ at 2 K, 10 K, and 300 K. The inset shows the derivative, dM/dH, which reveals the field-induced transition at 2 T and 5 T. (b) shows the M(H) of $Co_{0.9}Mg_{0.1}Ta_2O_6$ at 2 K, 10 K, and 300 K. The inset shows a field-induced transition present at 1 T. (c) shows the M(H) of x=0.3, 0.5, and 0.7 at 2 K. Field-induced transitions are absent for these compositions.

Figure 5 shows the isothermal magnetization curves, M(H), of the Co_{1-x}Mg_xTa₂O₆ compounds at different temperatures. Figure 5(a) shows the isothermal magnetization curves of CoTa₂O₆ at 2 K, 10 K, and 300 K. The M(H) plots are indicative of the antiferromagnetic nature of the compound. At 2 K, field-dependent transitions are present in CoTa2O6, which are evident in the derivative plot of dM/dH which is shown in the inset of Fig. 5(a). Critical field values $H_c \approx 2 \, T$ and $5 \, T$ can be identified. Figure 5(b) shows the magnetization isotherms of $Co_{0.9}Mg_{0.1}Ta_2O_6$ at 2 K, 10 K, and 300 K. Similar to the case of CoTa₂O₆, the field-induced transitions are present here as well but only at $H_c \approx 1$ T. As the content of Mg increases in the Co_{1-x}Mg_xTa₂O₆ series, the metamagnetic transition vanishes. As can be seen from Fig. 5(c), the magnetization curves acquire a weakly ferromagnic-like curvature for the compositions Co_{0.7}Mg_{0.3}Ta₂O₆, Co_{0.5}Mg_{0.5}Ta₂O₆, and Co_{0.3}Mg_{0.7}Ta₂O₆, however, sharp field-induced transitions are absent. Our magnetization data provide the indication of weak ferromagnetism induced by the clusters of broken Ising spins in the chain-like structure which otherwise forms an antiferromagnetic structure. Detailed studies involving neutron scattering and specific heat are underway to elucidate the details of magnetic structure and the magnetic excitations.

IV. CONCLUSIONS

Introducing diamagnetic Mg in the Co lattice of $CoTa_2O_6$ is observed to have three interesting effects: (i) the broad feature in magnetization that arises from the low dimensionality is suppressed, (ii) a large irreversibility is observed at 28 K in the magnetization of x=0.1, which also displays additional anomalies at low temperature, and (iii) a weak ferromagnetic component in the magnetization of x=0.5 and 0.7 is enhanced. The magnetization response as a function of temperature could be modeled after anisotropic Heisenberg or as Ising interactions in a chain, confirming the low dimensional behavior in these systems. Our study suggests the possibility of forming a weak ferromagnetic component in otherwise Ising-like chains and offers the possibility of studying these systems from the perspective of single-chain molecule systems realized in oxides.

ACKNOWLEDGMENTS

H.S.N. acknowledges the start-up grant from UTEP. L.M.M. and S.R.S. also acknowledge UTEP start-up funds. L.M.M. acknowledges LSAMP Ph.D. fellowship.

REFERENCES

¹N. Samarth, Nature **546**(7657), 216 (2017).

²A. B. Christian, A. Rebello, M. G. Smith, and J. J. Neumeier, Phys. Rev. B **92**(17), 174425 (2015).

³A. B. Christian, S. H. Masunaga, A. T. Schye, A. Rebello, J. J. Neumeier, and Y.-K. Yu, Phys. Rev. B **90**(22), 224423 (2014).

⁴A. B. Christian, A. T. Schye, K. O. White, and J. J. Neumeier, J. Phys. Condens. Matter **30**(19), 195803 (2018).

⁵E. M. L. Chung, M. R. Lees, G. J. McIntyre, C. Wilkinson, G. Balakrishnan, J. P. Hague, D. Visser, and D. McK Paul, J. Phys. Condens. Matter **16**(43), 7837 (2004).

- ⁶E. J. Kinast, V. Antonietti, D. Schmitt, O. Isnard, J. B. M. da Cunha, M. A. Gusmao, and C. A. Dos Santos, Phys. Rev. Lett. 91(19), 197208 (2003). ⁷D. T. Maimone, A. B. Christian, J. J. Neumeier, and E. Granado, Phys. Rev. B 97(10), 104304 (2018).
- ⁸A. Golubev, R. E. Dinnebier, A. Schulz, R. K. Kremer, H. Langbein, A. Senyshyn, J. M. Law, T. C. Hansen, and H.-J Koo, Inorg. Chem. 56(11),
- ⁹N. Matsubara, F. Damay, B. Vertruyen, N. Barrier, O. I. Lebedev, P. Boullay, E. Elkaïm, P. Manuel, D. D. Khalyavin, and C. Martin, Inorg. Chem. 56(16), 9742-9753 (2017).
- ¹⁰R. K. Kremer and J. E. Greedan, J. Solid State Chem. 73(2), 579–582 (1988). ¹¹R. K. Kremer, J. E. Greedan, E. Gmelin, W. Dai, M. A. White, S. M. Eicher, and K. J. Lushington, J. Phys. Colloques 49(C8), C8-1495 (1988).
- 12J. M. Law, H.-J. Koo, M.-H. Whangbo, E. Brücher, V. Pomjakushin, and
- R. K. Kremer, Phys. Rev. B 89(1), 014423 (2014). ¹³Takano Mikio and Takada Toshio, Mater. Res. Bull. **5**(6), 449–454 (1970).
- ¹⁴J. N. Reimers, J. E. Greedan, C. V. Stager, and R. Kremer, J. Solid State Chem. 83(1), 20-30 (1989).
- ¹⁵K. Momma and F. Izumi, J. Appl. Crystallogr. **41**(3), 653–658 (2008).
- ¹⁶E. J. Kinast, C. A. Dos Santos, D. Schmitt, O. Isnard, M. A. Gusmao, and J. B. M. da Cunha, J. Alloys Comp. 491(1-2), 41-44 (2010).
- 17A. Rebello, M. G. Smith, J. J. Neumeier, B. D. White, and Y.-K. Yu, Phys. Rev. B 87(22), 224427 (2013).
- ¹⁸F. D. M. Haldane, J. Phys. C Solid State Phys. **14**(19), 2585 (1981).
- ¹⁹F. D. M. Haldane, Phys. Rev. B **25**(7), 4925 (1982).

- 20 E. Pytte, Phys. Rev. B 10(5), 2039 (1974).
- ²¹E. Pytte, Phys. Rev. B **10**(11), 4637 (1974).
- ²²M. C. Cross and D. S. Fisher, Phys. Rev. B **19**(1), 402 (1979).
- ²³Md M. Seikh, V. Caignaert, O. Perez, B. Raveau, and V. Hardy, Phys. Rev. B 95(17), 174417 (2017).
- ²⁴V. Antonietti, E. J. Kinast, L. I. Zawislak, J. B. M. da Cunha, and C. A. dos Santos, J. Phys. Chem. Solids 62(7), 1239-1242 (2001).
- ²⁵H. M. Rietveld, J. Appl. Crystall. 2(2), 65–71 (1969).
- ²⁶J. Rodriguez-Carvajal, see https://www.ill.eu/sites/fullprof/php/ downloads.html for the latest version of Fullprof Suite (2018).
- ²⁷S. M. Eicher, J. E. Greedan, and K. J. Lushington, J. Solid State Chem. 62(2), 220-230 (1986).
- 28V. D. Mello, L. I. Zawislak, J. B. Marimon da Cunha, E. J. Kinast, J. B. Soares, and C. A. dos Santos, J. Magn. Magn. Mater. 196, 846-847
- ²⁹Y. Muraoka, T. Idogaki, and N. Uryû, J. Phys. Soc. Jpn. **57**(5), 1758–1761
- (1988).

 30 J. P. Hague, E. M. L. Chung, D. Visser, G. Balakrishnan, E. Clementyev, D. McK Paul, and M. R. Lees, J. Phys. Condens. Matter 17(46), 7227 (2005).
- 31 A. Nag and S. Ray, J. Magn. Magn. Mater. 424, 93-98 (2017).
- 32T. Mousavand, T. Naka, K. Sato, S. Ohara, M. Umetsu, S. Takami, T. Nakane, A. Matsushita, and T. Adschiri, Phys. Rev. B 79(14), 144411
- ³³J. C. Bonner and M. E. Fisher, Phys. Rev. A **135**(3), A640 (1964).
- 34R. L. Carlin, Magnetochemistry (Springer Verlag, New York, 1986).